

Scientific paper

General tendencies of stable isotopes and major chemical constituents of the Dome Fuji deep ice core

Okitsugu Watanabe¹, Kokichi Kamiyama¹, Hideaki Motoyama¹, Yoshiyuki Fujii¹, Makoto Igarashi¹, Teruo Furukawa¹, Kumiko Goto-Azuma¹, Takashi Saito², Satoru Kanamori¹, Nobuko Kanamori¹, Naohiro Yoshida³ and Ryu Uemura³

¹National Institute of Polar Research, Kaga 1-chome, Itabashi-ku, Tokyo 173-8515

²Disaster Prevention Research Institute, Kyoto University, Gokasho, Uji 611-0011

³Tokyo Institute of Technology, Nagatsuda, Midori-ku, Yokohama 226-8502

Abstract: Stable isotope compositions of water and major chemical constituents of the Dome Fuji ice core are analyzed and the data sets over the entire depth of the 2503-m core are presented in appropriate time resolution as consecutive series of average value in definite terms. These results based on the first stage analyses allow a temporal climatic dividing of the three glacial-interglacial cycles present in the records. A comparison of the climatic and environmental characteristics of these climate stages is presented.

key words: Dome Fuji, ice core, stable isotope, chemical constituent, Antarctica

1. Introduction

The first successful deep ice core drilling at Camp Century, Greenland in 1966 had a strong impact on earth science. It was followed by another successful ice core drilling at Byrd station, west Antarctica in 1968. Deep ice core studies started in several places on the Antarctic and Greenland ice sheets after these successes.

The Antarctic ice sheet preserves past global scale climate and environment signals in the snow and ice. These signals are linked to local temperature and precipitation rate, moisture source conditions by stable isotope ratios of oxygen and hydrogen in water molecules, and earth surface condition and general circulation strength by the flux and composition of primary and secondary aerosols from marine, terrestrial, cosmic and anthropogenic origins. Entrapped air inclusions provide direct records of past changes in atmospheric trace gas composition.

To construct a long term paleoclimate record, deep ice core drilling has been carried out at Byrd, Vostok, Dome C, and Law Dome in Antarctica.

The Vostok ice core data show that the atmospheric concentrations of greenhouse gases oscillated in close harmony with global temperature changes during the past several hundred thousand years (Barnola *et al.*, 1987; Petit *et al.*, 1999). In the Arctic, the GRIP (Greenland Ice-core Project; 1990–1992) core reveals 22 interstadial (warm) events during the last glacial period with very rapid warming and moderate cooling (Johnsen *et al.*, 1992).

A deep ice core drilling project was carried out during 1993–1998 at Dome Fuji,

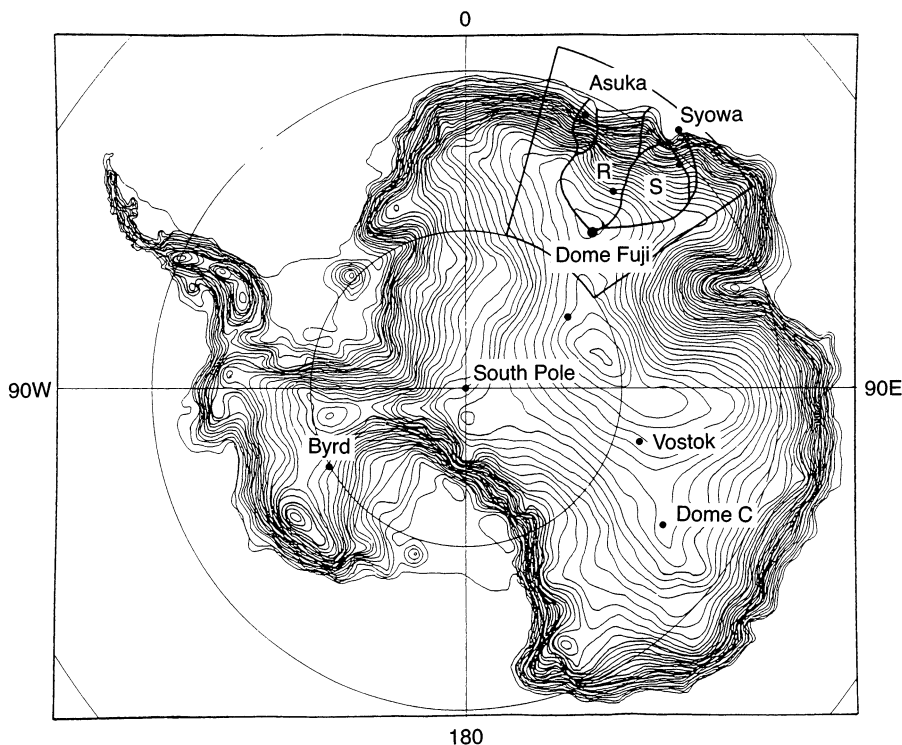


Fig. 1. Location of Dome Fuji drilling site in East Dronning Maud Land, Antarctica. S: Shirase drainage basin, R: Ragnhild drainage basin. Contour lines are drawn every 100 m. Dome Fuji Station; Location: $77^{\circ}19'01''\text{S}$, $39^{\circ}42'12''\text{E}$; Altitude: 3810 m a.s.l.; Ice thickness: 3028 ± 15 m.

Antarctica, as a part of a comprehensive glaciological study to clarify the present and past glaciological and climate condition of the Antarctic Ice Sheet in East Dronning Maud Land (Watanabe *et al.*, 1997a, b).

Deep ice core drilling was carried out to a depth of 2503.52 m in 1996 at Dome Fuji, which is one of the principal summits of the ice sheet in East Antarctica (Fig. 1).

This paper is a result of basic analysis of the Dome Fuji deep ice core. We present a series of detailed Dome Fuji records covering more than 320-kyr. In a full-depth core, the mean values of oxygen isotope content and main chemical concentration were obtained in uniform intervals (corresponding to equal numbers of years).

Climatic division in three glacial cycles has been determined from the profiles of oxygen isotope composition, of concentrations of the principal chemical components and of atmospheric gas composition. The environmental characteristics of each climatic division are described in terms of concentrations of the principal chemical constituents and atmospheric trace gases.

2. Geographic and climatic conditions of the Dome Fuji area

Dome Fuji is the second highest summit area of the Antarctic ice sheet (excluding coastal mountains). A JARE inland traverse party found the location of the top in 1985

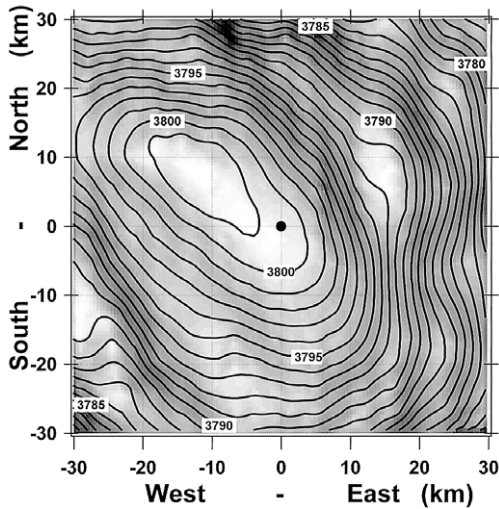


Fig. 2. Surface topography of Dome Fuji area (S. Fujita, unpublished).

• : Location of Dome Fuji Station. Numerals: Altitude, m a.s.l

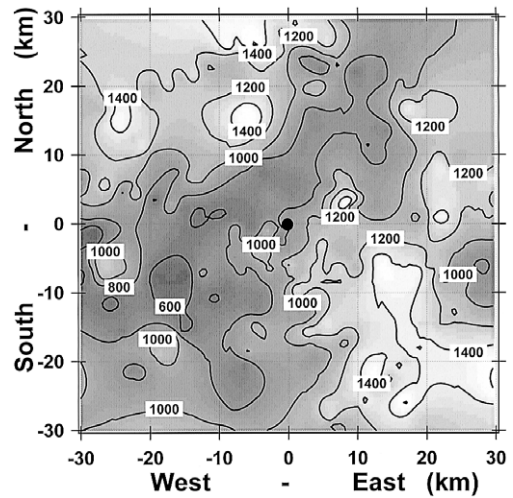


Fig. 3. Bedrock topography of Dome Fuji area (S. Fujita, unpublished).

• : Location of Dome Fuji Station. Numerals: Altitude, m a.s.l.

(Ageta *et al.*, 1989).

The surface topography of the Dome Fuji area is very smooth and flat as shown in Fig. 2; surface elevations around 30 km from the dome summit are only 7 m to 30 m lower than at the summit, with a mean of some 20 m at that distance. The mean surface slope in the circle of radius 30 km is estimated at about 1/1500. A topographical map of the bedrock around Dome Fuji is shown in Fig. 3.

The location of Dome Fuji Station (drilling site) was decided on the basis of both surface and bedrock topographies. The station is situated above relatively flat bedrock about 800 m in altitude. The bedrock topography around the dome exhibits what appears to be a saddle point. Bedrock hills higher than 1000 m a.s.l. are located to the southeast and northwest, and lowlands lower than 600 m a.s.l. are located to the west.

The ice thickness at the Dome summit was measured by detailed radar echo soundings to be 3028 ± 15 m in 1996 (Watanabe *et al.*, 1999).

Atmospheric pressure, air temperature, wind direction, wind speed and global solar radiation were observed by the JARE wintering teams from 1995 to 1997 (Japan Meteorological Agency, 1996, 1997, 1998). These data except global solar radiation are shown in Fig. 4. From March 1995 to December 1997, an annual mean air temperature of -54.3°C at 1.5 m height was recorded. The lowest recorded temperature for this period, -79.7°C , occurred on 14 May 1996 and 8 July 1997. Annual mean atmospheric pressure was 598.4 hPa, and annual mean wind speed at 10 m height was 5.8 m s^{-1} . The most frequent wind direction was northeasterly, but this accounted for only 15% of the total.

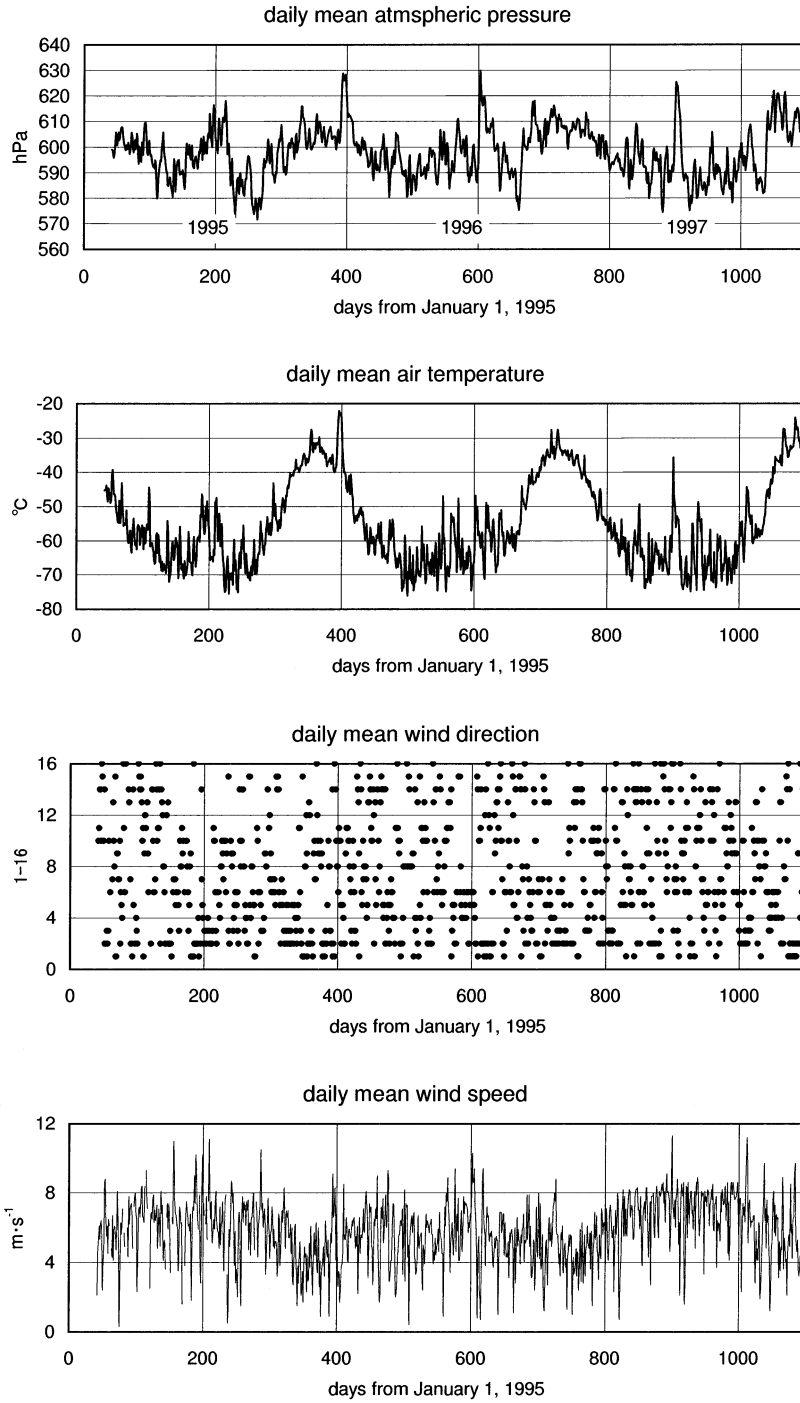


Fig. 4. Meteorological data at Dome Fuji Station during 1995–98. From top, daily mean atmospheric pressure (hPa), air temperature ($^{\circ}\text{C}$), wind direction (1-16) and wind speed ($\text{m}\cdot\text{s}^{-1}$).

3. Glaciological conditions of the Shirase drainage basin and Dome Fuji area

Dome Fuji is upstream of the Shirase drainage basin (Fig. 1) where glaciological research has been conducted by JARE inland traverse teams in the last 10 years. Glaciological data such as surface elevation, ice thickness, surface ice flow velocity, snow accumulation, snow temperature vs. depth profile, surface snow stratigraphy, isotopic and chemical characteristics of surface snow cover have been observed along the traverse route from the coast to the Dome Fuji area.

The spatial distribution of oxygen isotopic composition and major chemical constituents of the snow cover along the traverse route from the coast to the Dome area are shown in the Folio series (National Institute of Polar Research, 2001).

Observations of snow depositional characteristics at Dome Fuji have been conducted in the period 1995–1997 as well. The average surface mass balance ($3.2 \text{ g cm}^{-2} \text{ a}^{-1}$) in this area was estimated in 1989 using the 1963 tritium peak horizon (Kamiyama *et al.*, 1989). An annual surface mass balance of $2.5 \pm 1.0 \text{ g cm}^{-2} \text{ a}^{-1}$ was found for the measurement period 25 January 1995 to 31 January 1996. More than 95% of the surface mass balance (2.4 g cm^{-2}) was accounted for by the period February to mid-October. The surface mass balance for the rest of the year was reduced (0.1 g cm^{-2} for the period mid-October–January) due to strong sublimation during the summer months. In total during 1995, the sublimation process subtracted ~6% ($0.16 \text{ g cm}^{-2} \text{ a}^{-1}$) from the surface mass balance. Measurements of the vertical distribution of snow temperature through 1995 revealed an average 10 m-depth temperature of -57.3°C .

The seasonal distribution of $\delta^{18}\text{O}$ in the surface snow at Dome Fuji is in the range -45% to -75% , increasing in summer and decreasing in winter, as shown in Fig. 5. Judging from Fig. 5, concentrations of Na^+ and Cl^- in surface snow increased in spring-early summer. Those of MSA^- and SO_4^{2-} attained maximum values in spring and late autumn, then decreased in late summer and winter. NO_3^- showed increasing trends in early summer and late winter. Cl^-/Na^+ increased in summer. Stratigraphic observations, density measurements and snow sampling for chemical analyses were conducted in 2–3 m deep snow pits in each year during 1995–2000. A distinct structure consisting of stratified layers composed of alternately hard packed and loose snow is observed in the deposited snow at Dome Fuji Station. The hard layers are composed of a mixture of compacted snow and hard-type depth hoar. The loose layer is skeleton-type depth hoar. Vertical profiles of major chemical concentrations in the surface layers are shown in Fig. 6. These profiles suggest the occurrence of chemical migration processes in the surface snow layer. Na^+ , Cl^- and SO_4^{2-} show no remarkable change with depth. An abrupt decrease of NO_3^- and MSA^- concentration is present near 30 cm in depth from the surface.

4. *In-situ* procedure

The *in-situ* core analyses consist of electrical conductivity measurements (ECM), stratigraphic observations and bulk density measurements were carried out. ECMs include both DC and AC measurements. Stratigraphic observations include careful examination of tephra layers, cloudy bands and air bubbles/clathrate hydrates.

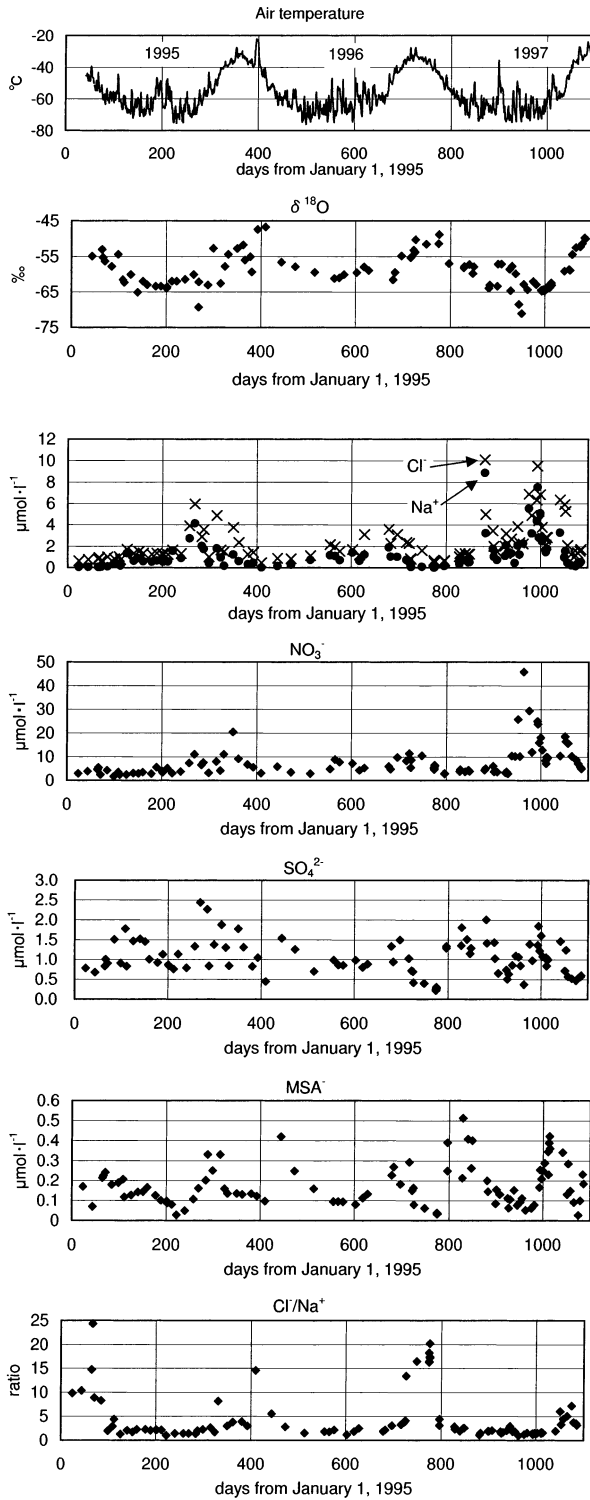


Fig. 5. Seasonal variation of oxygen isotope composition, major chemical concentrations (Cl^- , Na^+ , NO_3^- , SO_4^{2-} , MSA^-) and Cl^-/Na^+ at Dome Fuji Station during 1995–98. Daily mean air temperature is shown at the top of the figure.

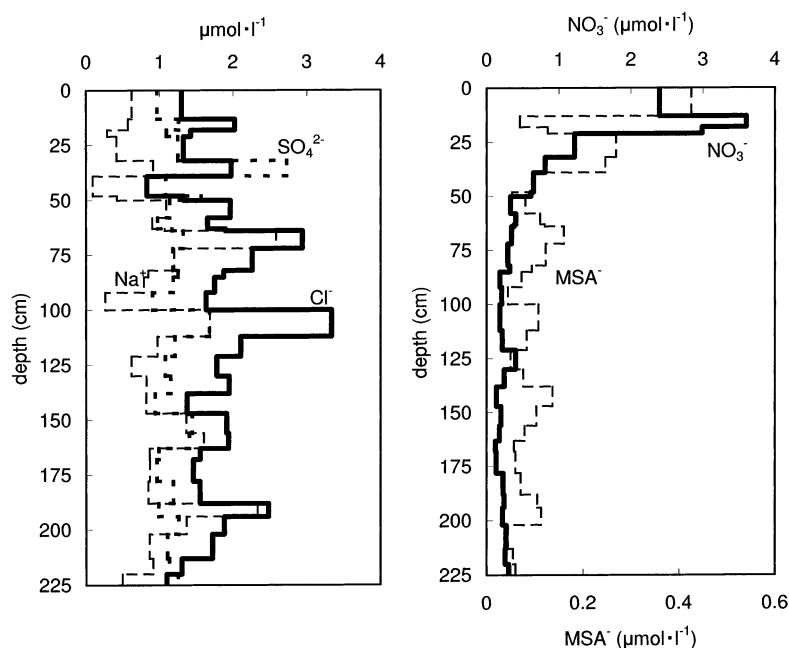


Fig. 6. Vertical profile of major chemical concentrations (Cl^- , SO_4^{2-} , Na^+ , NO_3^- and MSA^-) in the surface layer at Dome Fuji Station on December 26, 1997. Snow layer from the surface to 2.5-m deep contains about 25 annual layers.

After ice core retrieval, the cores were first stored in a storage trench for 1 to 4 months. Then they were processed. In the processing line, first the core sections were logged and bulk density measurements were made. Then the cores were cut parallel to the core axis into parts of 60% and 40%. The cut surfaces of the 60% parts were used for AC-, DC-ECM, and stratigraphic observations. At the end of the core processing line, cores were finally cut into three pieces along the core axis: 60% (A core); 25% (B core) and 15% (C core) (Fig. 7), and cut at every 50 cm for packing. Room temperature was normally kept at around -20°C for the ECM measurements.

Twenty-five tephra layers were observed in the core down to 2503 m (Fujii *et al.*, 1999). Two of these layers were found between 500 m and 600 m, and the remaining 23 were located below 1000 m, down to 2503 m. The layer thickness is in the range from 1 to 22 mm.

The cores were brittle at depths between some 500 m to 840 m. The starting depth of the brittle zone was roughly the same as the depth at which the first cloudy bands and clathrate hydrate crystals appeared. More than 700 distinct cloudy bands were found as well as many ambiguous layers. Most of the layers were located at three depth ranges, around 550 m, 1000 m and 2000 m and visible layer were rare at other depth ranges. Visible air bubbles have not been observed at depths below about 1100 m.

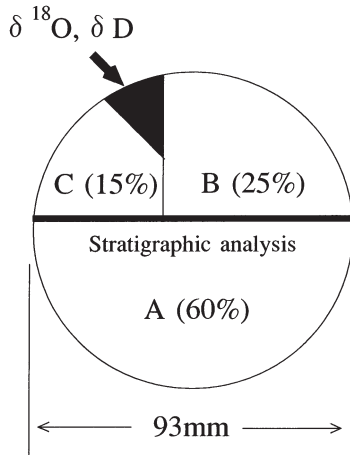


Fig. 7. Core cutting plan and item of core analyses.

A core (60%): Preservation part for future analyses; Analysis of atmospheric components.

B core (25%): Non destructive analyses; Stratigraphic analyses, physical properties, mechanical properties.

C core (15%): Melting and consumption analysis; Stable isotope analyses, chemical analyses, micro-particle analyses.

5. Oxygen isotope analyses

5.1. Oxygen measurements

The stable isotope composition of water ($\delta^{18}\text{O}$ and δD) is the most important element of the ice core study. The isotope composition is a function of the condensation temperature of vapor in the atmosphere, and the averaged $\delta^{18}\text{O}$ of the surface snow cover can be indicated in terms of the annual mean temperature which is approximately equal to the 10 m-depth snow temperature.

Systematic surface glaciological research has revealed a relationship between 10 m-depth snow temperature (T ; °C), and $\delta^{18}\text{O}$ (denoted by $\delta\text{‰}$) value. This relation is described as follows (Satow *et al.*, 1999).

$$\delta = 0.852 \times (T + 57.3) - 56.7.$$

The core dating (Watanabe *et al.*, 2003) is estimated using a flow model, which describes the thinning rate of the annual layer thickness. The annual layer thickness at the surface (accumulation rate) is estimated from $\delta^{18}\text{O}$ by an empirical equation using the present relationship between the accumulation rate (λ_0 ; cm of ice equivalent a^{-1}) and $\delta^{18}\text{O}$ from the Dome Fuji area higher than 3200 m a.s.l.:

$$\lambda_0 = 3.88 \exp(0.146(\delta + 55)).$$

To obtain a primary working time scale for the Dome Fuji core, continuous oxygen isotope measurements have been made on 25 or 50 cm-long samples (so called half or full bag samples) over the entire core depth. The measurements were performed on a Mat Delta E mass-spectrometer and the $^{18}\text{O}/^{16}\text{O}$ ratio obtained from each sample have been converted to $\delta^{18}\text{O}$, the relative deviation from that in standard mean ocean water. The total number of samples analyzed is about 8000.

After establishing an age-depth relation, 50-year averages of $\delta^{18}\text{O}$ data were calculated over the whole depth of the Dome Fuji core.

5.2. Oxygen isotope profile

The oxygen isotope profile from the surface to 110 m-depth was measured using a firn core drilled by shallow drilling. The measurement procedure was different from that used for the ice core: surface contamination was scrapped off the firn surface.

The results of the analyses are shown in Figs. 8 and 9, as profiles from the surface to 10 m-depth and a profile from the surface to 110 m-depth, respectively. The surface to 10 m-depth δ profile is composed of data obtained during 1993–1999 campaigns. In the upper part of the 1993 shallow core, the δ values cover the range $-62\sim-45\text{‰}$ with a tendency toward to higher δ near the surface (warmer temperature). To examine this tendency, closer sampling from the shallow cores and pit walls were performed near the station. Figure 8 shows that the surface profile obtained from the 1993 shallow core can be said to support this tendency. Also Fig. 8 indicates that the scattered δ distribution at the near surface is converging with depth due to depth hoar process caused by the intensive temperature gradient and mechanical packing in the surface snow cover.

Figure 9 shows $\delta^{18}\text{O}$ scattering in range of $-58\sim-50\text{‰}$. The thick line in Fig. 9 is the average value over 50 years with a mean of the value of -54.9‰ and this value has been applied as the present mean value of the Dome Fuji surface snow.

The Dome Fuji deep ice core record of oxygen isotopes from the surface to the depth of 2500 m is shown in Fig. 10. This figure is a combination of the 50-year $\delta^{18}\text{O}$ averages and a profile of the 1000-year running means (see Fig. 11).

This profile clearly shows three glacial interglacial cycles in a similar pattern to the

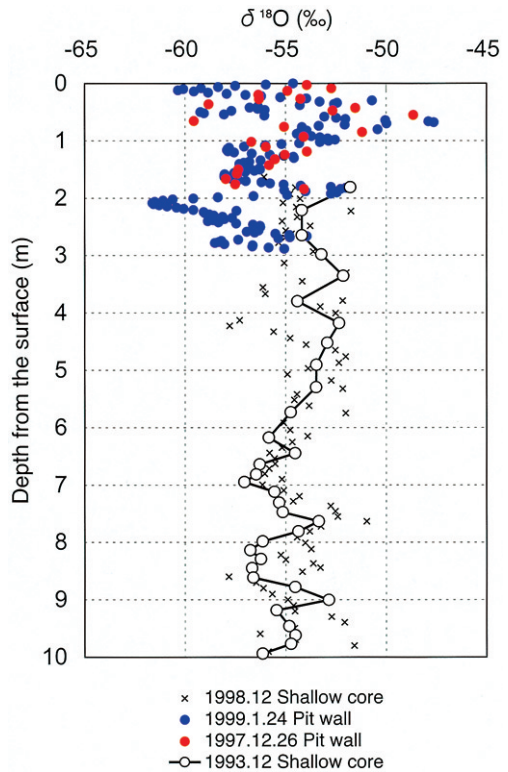


Fig. 8. Vertical profile of oxygen isotope composition from the surface to 10 m-depth (about 110 year before accumulation) at Dome Fuji Station. 0 m in depth means the snow surface in December 1993. Four sampling points were settled in a range of 200 m.

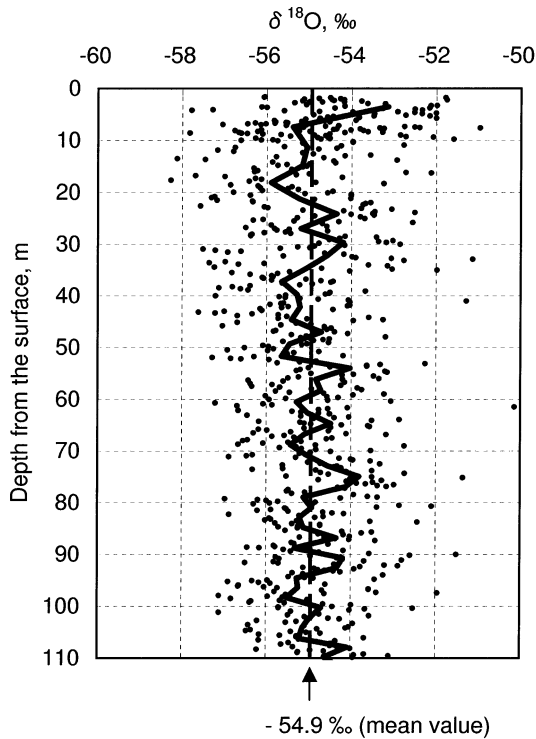


Fig. 9. Profiles of oxygen isotope composition of Dome Fuji shallow ice core from the surface to 110 m in depth. Solid circles mean the data of 10–20 cm long samples. The solid line means the 50-year average value.

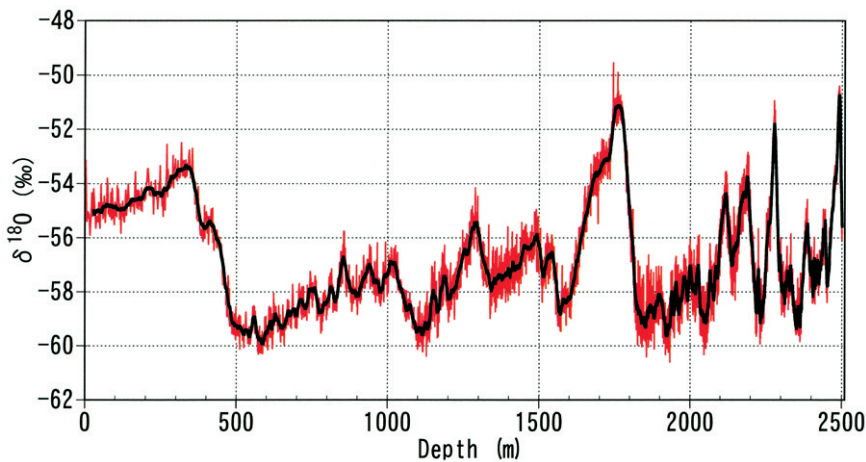


Fig. 10. Profile of oxygen isotope composition of Dome Fuji deep ice core from surface to 2503 m depth. Red thin line is 50-year averages. Black solid thin line means the 1000-year running mean value.

Vostok δD profile. Petit *et al.* (1999) noted that all four climate cycles show the same “saw-tooth” sequence of a warm interglacial (Marine Isotope Stage: MIS:11, 3, 9.3, 7.5 and 5.5), followed by increasingly colder interstadial events, ending with a rapid return toward the next interglacial. Also the Dome Fuji $\delta^{18}\text{O}$ profile exhibits similar features.

The temperature difference between glacial minima and inter-glacial maxima is 6–8°C using the relation between annual air temperature and average $\delta^{18}\text{O}$ in surface snow cover. The maximum temperatures in the inter-glacial phases are different in each cycle.

6. Deuterium analysis

6.1. Deuterium measurement

The sampling intervals are about 2 m from the snow surface to 400 m depth (the average time resolution is about 70 years), about 3 m to 2000 m depth (300 years resolution), and about 1 m to 2503 m-depth (300 years resolution).

In order to obtain the Dome Fuji d-excess record, δD measurement has been performed. Hydrogen isotope ratios of ice core samples are determined by the isotope equilibrium method at Tokyo Institute of Technology. Equilibration time is more than one hour with three platinum catalyst beads (Hokko beads, Shoko Co., Ltd.). The d-excess value is significantly altered by the subtle δD change. Two reference waters has been used as working standards with values similar to the internationally accepted reference (VSMOW and SLAP), and results were corrected to accepted values by using these waters.

In order to estimate the long term standard uncertainty of the δD measurements in the laboratory, a laboratory standard (distilled tap water with $\delta\text{D}=-62.3\text{‰}$) was constantly measured. The standard deviation (1σ , $n=330$) from results of the repeated analyses of the laboratory water standard over a year is $\pm 0.43\text{‰}$.

6.2. Deuterium excess record

The deuterium excess (d-excess) that is defined as $\text{d-excess}=\delta\text{D}-8\delta^{18}\text{O}$ (Dansgaard, 1964) indicates conditions of evaporation from the ocean surface. This definition is derived from a global scale linear relationship between deuterium and oxygen-18 composition of water (expressed as “ $\delta\text{D}=8\delta^{18}\text{O}+10$ ”, Craig, 1961). Although the global average d-excess is about 10, the d-excess of individual precipitation value shows significant variations. The variations of d-excess of each precipitation value are mainly caused by changes in evaporation conditions such as SST (sea surface temperature), humidity, and wind speed above the vapor source, ocean surface (Merlivat and Jouzel, 1979). Therefore, a d-excess record recovered from an ice core potentially has unique information on the sea surface condition of the water vapor source areas.

Figure 11 shows the Dome Fuji ice core records of δD and d-excess with the $\delta^{18}\text{O}$ profile. The δD values of the Dome Fuji core range from -390‰ to -470‰ . Although the d-excess record oscillates, most of the record ranges from 8‰ to 16‰ . The δD and d-excess records are clearly distinct in the short-period oscillation, but the δD record is smoother. This may partly be attributed to the larger analytical error of the d-excess.

The d-excess record shows three periodic glacial-interglacial changes, which differ from the δD and $\delta^{18}\text{O}$ records. For instance, d-excess value is high (from 13 to 16) during the first half of the last glacial period (from about 110 kyr BP to 70 kyr BP), and low (from 10 to 14) during the latter half of the period (from about 70 kyr BP to 20 kyr BP). A similar d-excess trend has been observed in the Vostok ice core (Vimeux *et al.*, 2001), and detailed comparison of the d-excess record of Dome Fuji and Vostok will provide additional information about changes in the origin of precipitation (Watanabe *et al.*, 2003)

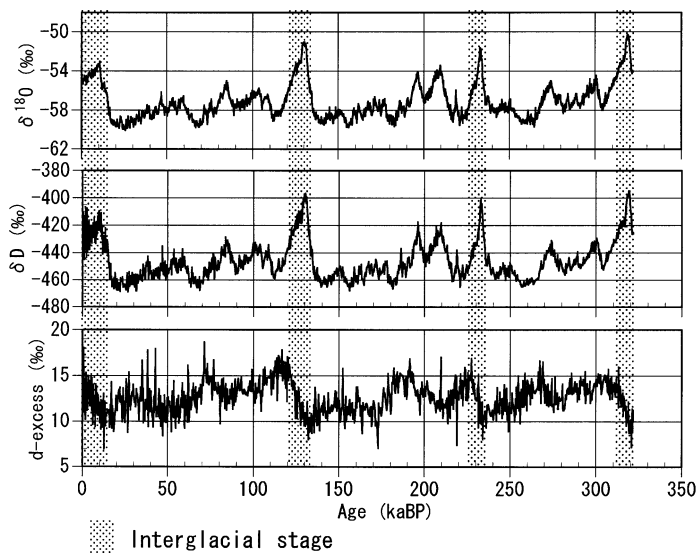


Fig. 11. Stable isotope composition ($\delta^{18}\text{O}$ and δD) and d -excess profile of Dome Fuji core. The $\delta^{18}\text{O}$ profile shows the 1000-year running mean. Intervals of δD and d -excess are described in the text.

7. Chemical analyses

7.1. Sample preparation and data processing

Basic analyses of major chemical species were carried out using 7–10 cm ice samples cut out of the 50 cm-long “bag samples” spaced from 0.5 to 2.5 m. Then data with 200-year resolution were established by the depth-age relationship for the entire depth of the Dome Fuji ice core. The total number of samples analyzed was about 3550. For comparison of the chemical data to the $\delta^{18}\text{O}$ data, both data set were transformed to the same time-scale.

The 7–10 cm long chemical samples were prepared in a cold room. Three mm of the surface part was scraped off to remove contamination by a ceramic knife in a clean-bench in a cold laboratory. The ice samples were stored in a plastic bag, and just before the melting and measurements they are rinsed with ultra-pure water (with an electrical resistance higher than 18.3 M Ω).

The firm samples were stored in a Teflon bottle and melted just before the measurements as reported by Watanabe *et al.* (1997).

The chemical analysis of the melted ice sample was done by ion-chromatograph Dionex DX-500 (isocratic system for cations and gradient system for anions).

The measured ions were Na^+ , NH_4^+ , K^+ , Mg^{2+} , Ca^{2+} , F^- , Cl^- , SO_4^{2-} , NO_2^- , NO_3^- , HCOO^- , CH_3COO^- , $\text{C}_2\text{O}_4^{2-}$, PO_4^{3-} and CH_3SO_3^- .

The vertical profiles of major chemical constituents are shown in Fig. 12. Remarkably high values were checked for possible contamination and/or improper sample treatment, and either excluded from the general plot, or measured again if possible.

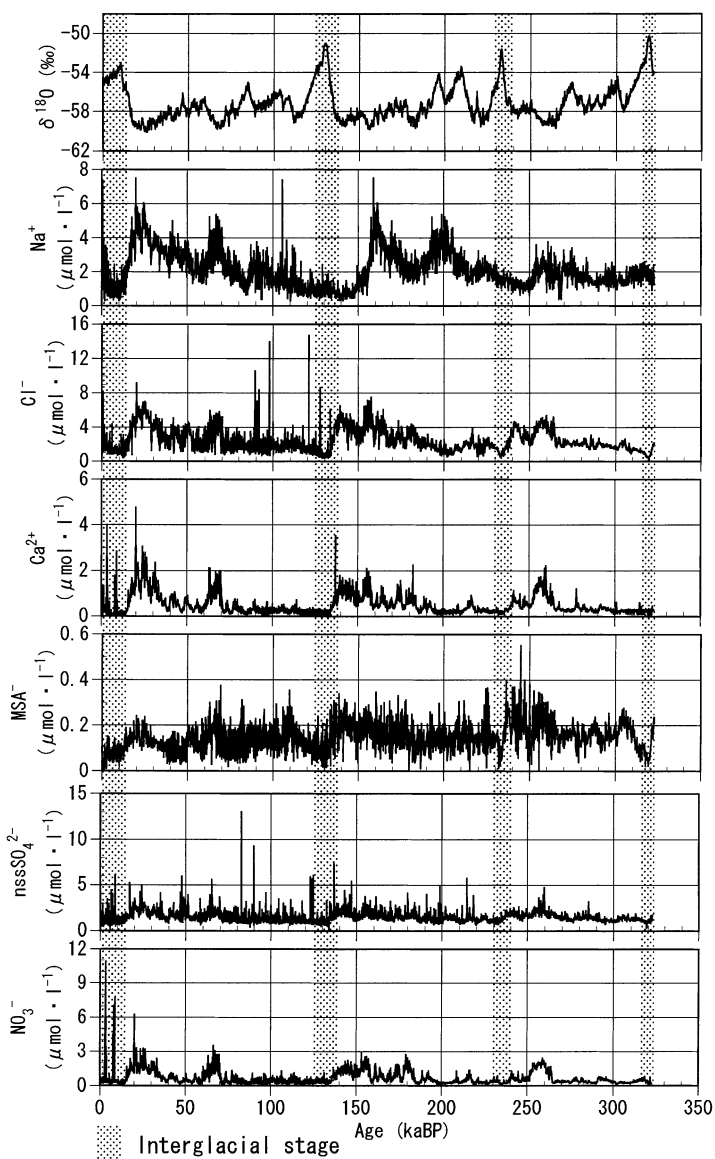


Fig. 12. Profiles of the concentration of $\delta^{18}O$ and major chemical species (Cl^- , Ca^{2+} , MSA^- , $nssSO_4^{2-}$ and NO_3^-) in the Dome Fuji core. Data intervals are 200 years.

7.2. Distribution and behavior of chemical constituents

7.2.1. Correlations of the major chemical constituents

Correlation analysis among eleven anions as well as non-sea-salt (nss) SO_4^{2-} and five cations was carried out. The correlation matrix is given in Table 1.

Correlation coefficients higher than 0.8 are found in 8 sets, and values higher than 0.7 in another 11 sets. Among the major chemical constituents of sea-salt related species (Cl^- ,

Table 1. Correlation matrix of the major chemical concentrations of the Dome Fuji deep ice core.

	CH ₃ COO ⁻	HCOO ⁻	MSA ⁻	Cl ⁻	NO ₂ ⁻	NO ₃ ⁻	SO ₄ ²⁻	C ₂ O ₄ ²⁻	PO ₄ ²⁻	Na ⁺	NH ₄ ⁺	K ⁺	Mg ²⁺	Ca ²⁺
F ⁻	0.76	0.74	0.29	0.14	0.71	-0.06	0.16	0.31	0.11	0.13	0.22	0.07	0.03	0.21
CH ₃ COO ⁻		0.78	0.43	0.32	0.70	0.17	0.32	0.23	-0.01	0.26	0.24	0.24	0.24	0.32
HCOO ⁻			0.27	0.13	0.64	0.06	0.04	0.54	0.10	0.11	0.51	0.00	-0.05	0.17
MSA ⁻				0.73	0.44	0.44	0.51	0.08	-0.06	0.62	-0.09	0.37	0.53	0.58
Cl ⁻					0.22	0.68	0.77	0.09	0.09	0.90	0.12	0.71	0.82	0.86
NO ₂ ⁻						-0.10	0.22	0.36	0.24	0.14	0.06	-0.04	0.02	0.27
NO ₃ ⁻							0.66	0.29	-0.20	0.76	0.04	0.59	0.81	0.60
SO ₄ ²⁻								0.13	0.01	0.83	0.01	0.65	0.92	0.81
C ₂ O ₄ ²⁻									0.13	0.17	0.38	-0.08	0.10	0.19
PO ₄ ²⁻										0.02	0.14	0.06	-0.09	0.19
Na ⁺											0.10	0.65	0.89	0.76
NH ₄ ⁺												0.09	-0.01	0.16
K ⁺													0.68	0.74
Mg ²⁺														0.72

SO₄²⁻, Na⁺, Mg²⁺, Ca²⁺, K⁺), higher correlations are found in the following 6 sets: Na⁺-Cl⁻ (0.90), Na⁺-SO₄²⁻ (0.83), Na⁺-Mg²⁺ (0.89), Cl⁻-Ca²⁺ (0.86), Cl⁻-Mg²⁺ (0.82), and Mg²⁺-SO₄²⁻ (0.81). These high coefficients indicate a significant contribution of the sea-salt to glacier ice, and at the same time, suggest an important effect of non-sea-salt deposition. Among these sea salt components, SO₄²⁻ in Antarctic snow and ice is mainly of biogenic sulfur origin and a part of the Mg²⁺, Ca²⁺, and K⁺ is of terrestrial origin. In this report, the sea-salt derived part is temporarily evaluated referring to Na⁺, assuming all Na⁺ is of sea-salt origin.

Legrand and Delmas (1988) report that Na⁺ partly derives from terrestrial dust (Legrand and Delmas, 1988).

The extent of the non-sea-salt contribution can be evaluated from Fig. 13. The bigger the gap between clusters of plotted points and the sea-salt ratio line, the higher the contribu-

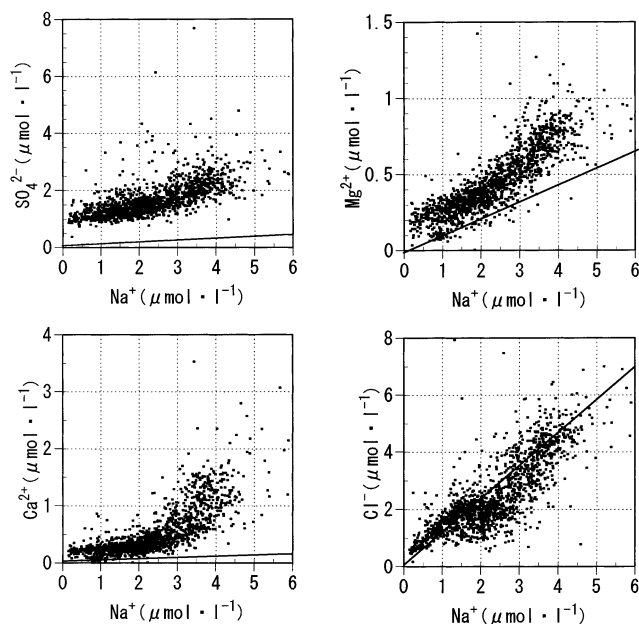


Fig. 13. Relation between Na⁺ and some chemical species (SO₄²⁻, Cl⁻, Mg²⁺, Ca²⁺). Solid lines are relations in sea water.

tion from other sources. The contribution from SO_4^{2-} is most evident, significant parts of Mg^{2+} and Ca^{2+} are of non-sea-salt origin and Cl^- shows complex behavior against Na^+ .

7.2.2. Relation between chemical concentrations and oxygen isotopic composition

Profiles of major chemical constituents (Na^+ , Cl^- , Ca^{2+} , MSA , nssSO_4^{2-} and NO_3^-) along the Dome Fuji core are shown in Fig. 12. These concentration profiles confirm that deposition of chemical constituents of marine and terrestrial origin are higher during cold climatic conditions than during the warm interglacials. The higher deposition is probably linked to higher meridional atmospheric circulation, more extensive arid areas and greater exposure of continental shelves under cold climate condition (Legrand *et al.*, 1988), which is exhibited as low $\delta^{18}\text{O}$ in the δ -records.

In the present paper, chemical concentrations are plotted against $\delta^{18}\text{O}$ value to disclose the direct relationship between distribution of chemical constituents and atmospheric temperature. The relation between major chemical constituents and oxygen isotope composition can be classified into three groups (1)–(3), as seen in Fig. 14.

(1) Na^+ , Mg^{2+} and Cl^- group

The data plot of Na^+ , like that of Mg^{2+} (not shown), converges to a concaved curve as seen in Fig. 14a and the concentration increases with decreasing $\delta^{18}\text{O}$ value, and thus with

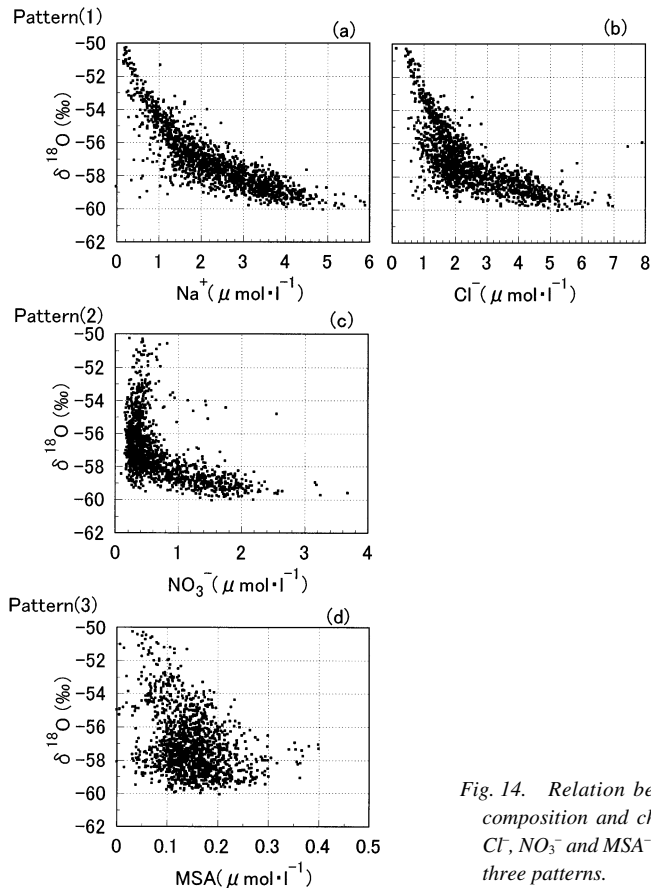


Fig. 14. Relation between oxygen isotope composition and chemical elements (Na^+ , Cl^- , NO_3^- and MSA). They are divided into three patterns.

decreasing temperature. This can be attributed to enhanced transportation by strengthened wind during the glacial cold period. The same plot of Cl^- , given in Fig. 14b, shows the same trend, but with some complex behavior, also Cl^- increases with decreasing $\delta^{18}\text{O}$ as Na^+ .

On the other hand, nssCl^- keeps constant low level in periods of higher $\delta^{18}\text{O}$ and decreases to negative values in periods of lower $\delta^{18}\text{O}$, with a minimum at about -57‰ (as seen in Fig. 15a). The presence of negative nssCl^- is also reported in the Vostok core and was ascribed to the formation of HCl gas from sea salt particles by reaction with $\text{H}_2\text{SO}_4^{2-}$ (Legrand *et al.*, 1988).

Further information is obtained from the Cl^-/Na^+ ratio plotted in Fig. 15b. The Cl^-/Na^+

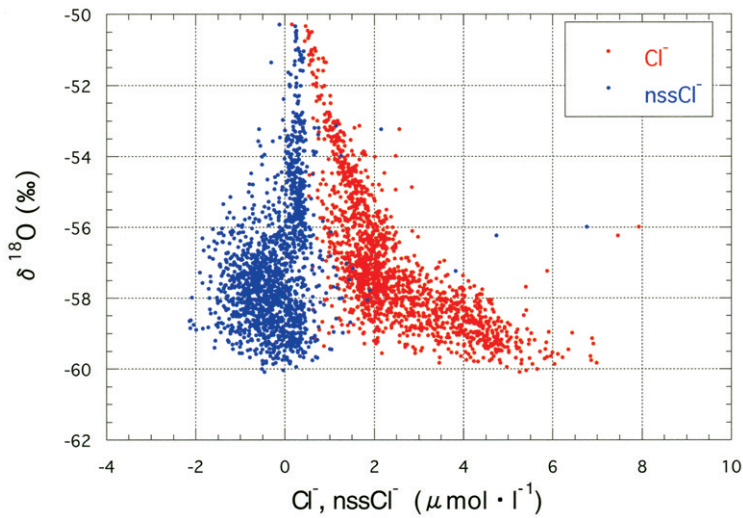


Fig. 15a. Relation between oxygen isotope composition ($\delta^{18}\text{O}$), Cl^- and nssCl^- .

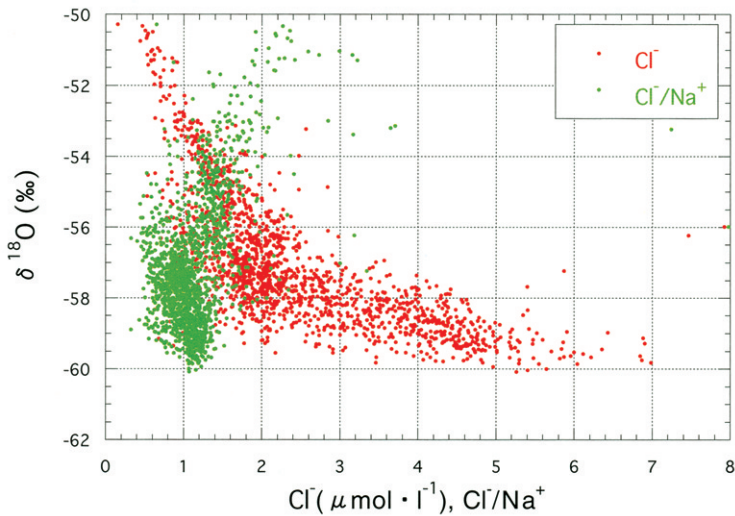


Fig. 15b. Relation between oxygen isotope composition ($\delta^{18}\text{O}$), Cl^- and Cl^-/Na^+ .

ratio increases with increasing $\delta^{18}\text{O}$ at range higher than -57‰ and indicates the formation of HCl from sea salt particles. In the lower range, on the contrary, the Cl^-/Na^+ ratio decreases to a minimum value at 1.0 or less and then increases to about 1.2, which is the Cl^-/Na^+ ratio in sea water. This points at a higher transportation and deposition rate of sea salt particles due to high wind speed without reaction with nssSO_4^{2-} (Legrand *et al.*, 1988).

According to the above considerations, the Cl^- concentration is mainly controlled by a chemical reaction process which is more active at warmer climate condition, whereas Cl^- at colder climate condition is controlled by physical processes with a switching point for the two processes around a $\delta^{18}\text{O}$ value of -57‰ .

(2) NO_3^- , SO_4^{2-} and Ca^{2+} group

The plot of concentration of these constituents against $\delta^{18}\text{O}$ can be treated as a combination of two different curves: the upper one, which leads to higher concentration with increasing temperature, and the lower one, which leads to progressively higher concentration toward the coldest climate. The latter is the same process as mentioned in (1); both combine at a $\delta^{18}\text{O}$ value about -57‰ . The case of NO_3^- is a typical one as shown in Fig. 14c. The increase in NO_3^- concentration with increasing temperature may due to higher activity of organisms on the earth surface, higher solar radiation and other causes. SO_4^{2-} and Ca^{2+} show similar behavior to NO_3^- but without the distinctive increase at higher temperature.

(3) MSA^- , NO_2^- , NH_4^+ and F^- group

These chemical constituents show broadly scattered profile patterns against $\delta^{18}\text{O}$ as shown in Figs. 14d. Low correlation coefficients are found. Most elements belonging to this group are derived through processes including gaseous reactions during transportation to the Antarctic inland region from their source area.

7.2.3. The relation between micro-particles and oxygen isotope composition

The numbers and volume concentrations of micro-particles are measured by setting the measurement range 10 to $0.52\text{--}5.04\ \mu\text{m}$. The number concentration of micro-particles in Dome Fuji core increases in the coldest phase during the glacial period as described in Watanabe *et al.* (1999). A detailed discussion of the measurement and the profile are presented by Fujii *et al.* (2003).

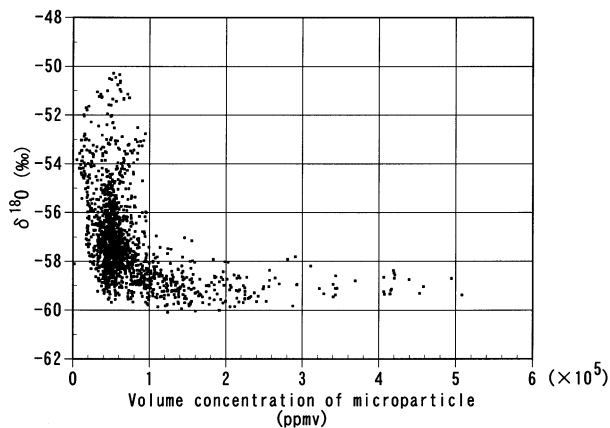


Fig. 16a. Relation between oxygen isotope composition ($\delta^{18}\text{O}$) and volume concentration of micro-particles ranges.

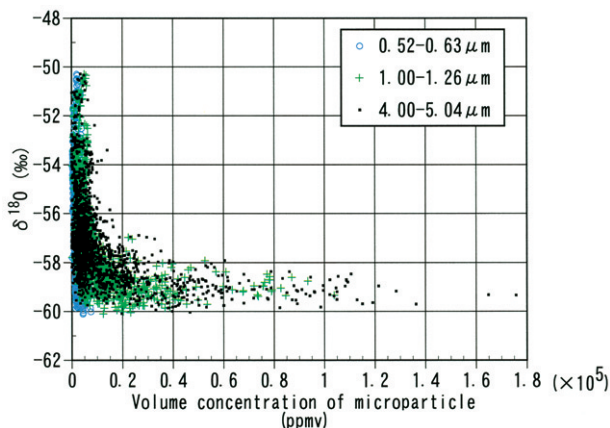


Fig. 16b. Relation between oxygen isotope composition ($\delta^{18}\text{O}$) and volume concentration of micro-particles classified into three particle sizes.

The relation between the total volume concentration and $\delta^{18}\text{O}$ is shown in Fig. 16a. As seen in this figure, the plot pattern resembles the pattern of most chemical constituents (1) in Fig. 14. The distribution pattern is a combination of a warmer climate pattern and a colder climate pattern.

The volume number of three particle size fractions (0.52–0.63, 1.00–1.26, and 4.00–5.05 μm) plotted versus $\delta^{18}\text{O}$ is shown in Fig. 16b. The sharp increase in particle volume in the coldest period is most evident with the largest size fraction and clearly indicates increased exposed area of continental shelf due to sea surface lowering and transportation of particles by high wind speed. This confirms that the process, which is active in a colder climate and induces a high load of impurity on the ice sheet, is supported by enhanced transportation of terrestrial aerosols.

8. Climatic and environmental division during the glacial–interglacial cycles

8.1. Climatic division of the glacial-interglacial cycle

In the previous section we examined the characteristics of climatic and environmental variation based on the profiles of continuous 50-year bulk averaged oxygen isotopic composition and major chemical concentration in 200-year resolution.

The entrapped air component in the core has been analyzed by a Tohoku University group, and the results are reported by Kawamura (2000) and Kawamura *et al.* (2003).

The 320 kyr $\delta^{18}\text{O}$ variation of the Dome Fuji deep ice core reveals three glacial-interglacial cycles. These cycles show similarities in general tendency and also differences if examined in detail. For detailed comparison of each climatic stage and its characteristics, climate dividing is essential.

Lorius *et al.* (1985) designated the successive warm and cold stages as A–H for the 160 kyr Vostok core. Starting from the top, the warm periods are designate by A, C, E and G and the cold periods by B, D, F and H. In their designation, stage A corresponds to the present Holocene period and Stage G is the last interglacial and stage H is the last part of the previous glacial. Though the definition of the stage boundary is not clear, it exhibit the interme-

diate between the highest and lowest temperatures in adjacent stages.

To do our climate dividing, we define the stage boundaries by comparison with the Vostok δD record. In our application, Stage A corresponds to the interglacial stage and the mark B-F corresponds to stadial and interstadial stages during a glacial period.

Petit *et al.* (1999) examined all glacial terminations and commencements using the data set of the past 420 kyr from Vostok core. The profiles of δD_{ice} , $\delta^{18}O_{atm}$, CO_2 , CH_4 and dust have been analyzed. According to their figure, which indicated time series of the elements during glacial terminations, the terminations of the past four glacial periods coincide with large decreases in dust concentration including a case of much earlier occurrence.

The climate events during the transition phases in the Dome Fuji core exhibit variations of $\delta^{18}O_{ice}$, $\delta^{18}O_{air}$ and CH_4 as shown in Fig. 17. Also the variations of major chemical concentrations, Na^+ , Ca^{2+} and SO_4^{2-} , as environmental signals, are shown in the figure.

In these glacial–interglacial cycles, similar trends of variation are found and among them remarkable stadial and interstadial stages show distinctive climate events. It is obvious

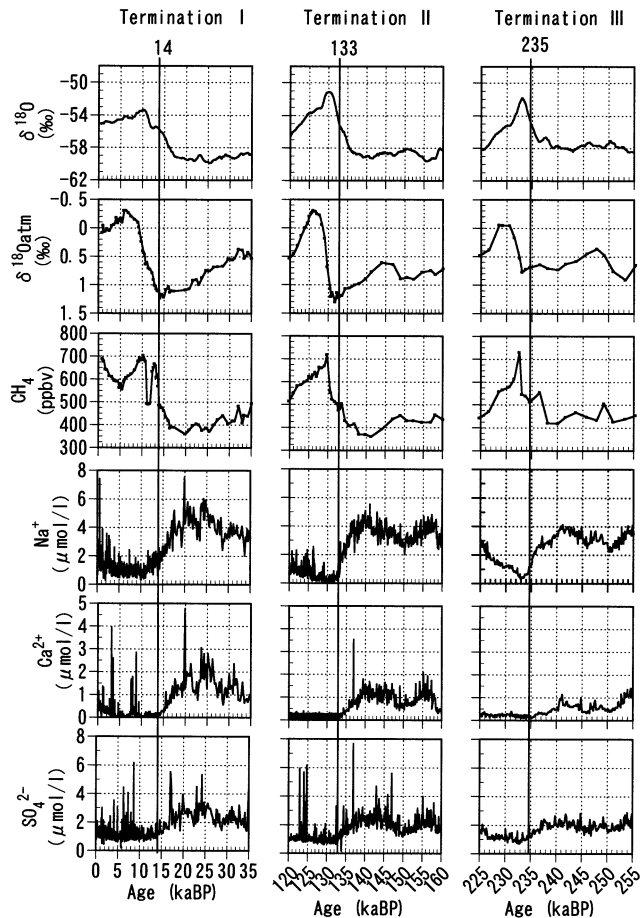


Fig. 17. Variation of climatic signals in the transition phase (Termination I–III). $\delta^{18}O_{ice}$, $\delta^{18}O_{atm}$, CH_4 , Na^+ , Ca^{2+} and SO_4^{2-} are shown in this figure.

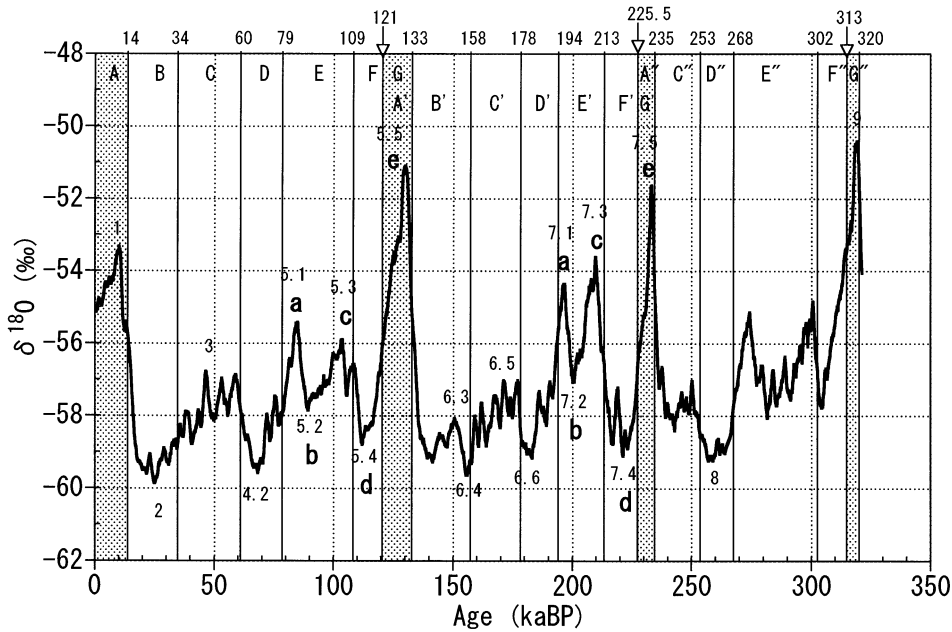


Fig. 18a. Temporal climatic division in the three glacial-interglacial cycle. Notations are described in this text.

from these figures, that concentration of Ca^{2+} , mainly from originated mainly from terrestrial areas, $\delta^{18}\text{O}_{\text{ice}}$ and SO_4^{2-} reached minimum levels about the same time. The minimum levels of Ca^{2+} and SO_4^{2-} indicate the completion of intense aerosol transportation from marine and land through highly developed air circulation during the glacial period. As to the Antarctic ice sheet, the completion of intense general circulation means the termination of a glacial period.

Using the termination timing estimated from comparison of the climatic and environmental signals as indicated in Fig. 17, a tentative climatic dividing of the glacial-interglacial cycles is proposed. Scheme of this dividing is indicated in Fig. 18a. In this figure, the climate division is designated by A–G; A and G are interglacial periods so that G is A' and G' is A''. Warm periods (interstadial) are A, C and E, and cold periods (stadial) are the same as in the usage of Lorius *et al.* (1985). Marine isotope stage numbers in this figure are tentative.

Average concentration value of the major chemical components in each stadial-interstadial stage are indicated as the line graph in Fig. 18b.

8.2. Comparison of environmental characteristics between the glacial-interglacial cycles

The Antarctic ice sheet preserves signals relating to global paleo-environmental and climatic changes in form of emission of substances and gases from various sources during the last some hundred thousand years. Those substances and gases were transported to the Antarctic ice sheet through general circulation of the troposphere and the stratosphere.

Substances originate from the ocean surface and marine bioactivities are transported to the Antarctic ice sheets through the lower troposphere by cyclonic disturbances. Dust from arid regions and exposed continental shelves is the most probable source for micro-particles

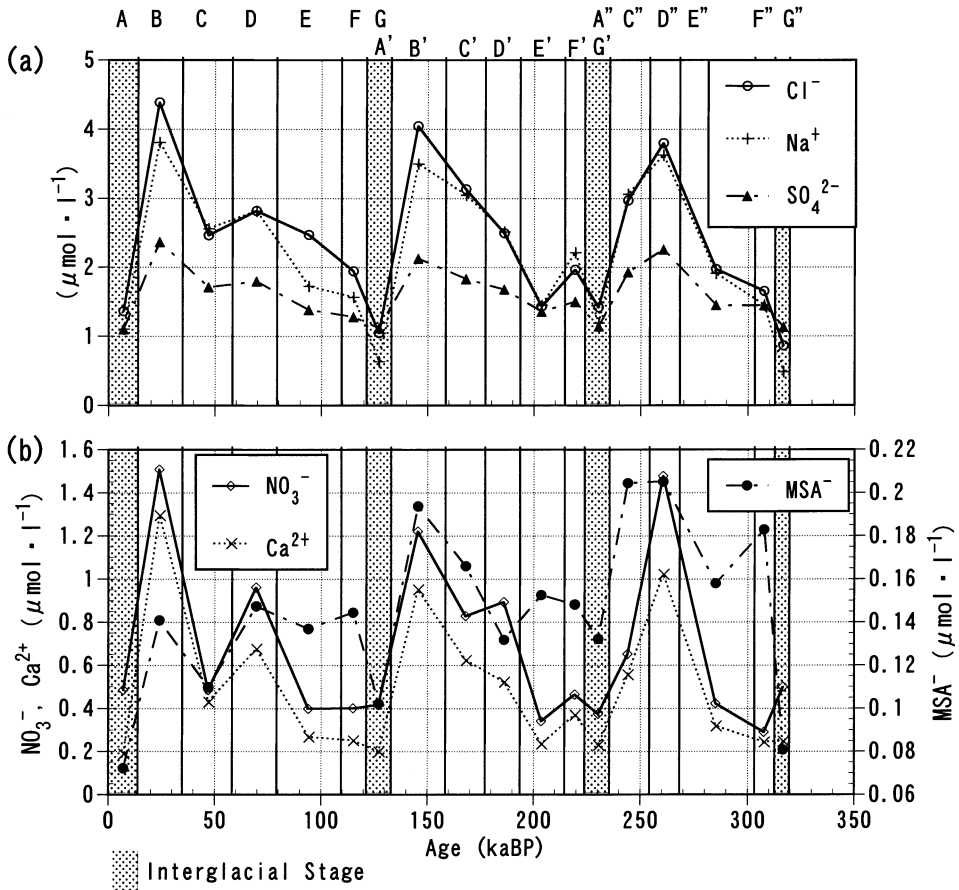


Fig. 18b. Variation in the averaged concentration of some chemical species in the stadial-interstadial stages. (a) Cl^- , Na^+ and SO_4^{2-} , (b) NO_3^- , Ca^{2+} and MSA^- .

in polar core. The concentration decreases with distance from the coast.

Transportation of trace gases and gas derived aerosols differs much from that of particulate matters; they are spread to the upper troposphere and the stratosphere. Subsidence of air masses of the upper troposphere and stratosphere is an important process at the inland plateau of the Antarctic ice sheet for gas derived aerosols and stratospheric substances such as nitrate and tritium (Kamiyama *et al.*, 1989).

The isotopic composition, major chemical concentrations and entrapped air constituents in the Dome Fuji deep ice core are examined to characterize variations during glacial and interglacial cycles. In particular, similarities and differences in the variation during stadial and interstadial stages are compared in detail.

As results from these studies, some of interesting phenomena are found and described;

(1) In general, a good correlation is found between concentrations of atmospheric gases, ions and $\delta^{18}O$ (temperature proxy). Typical examples are Na^+ and Cl^- (may be SO_4^{2-} also) as good indicators of wind velocity over the sea surface. In the first cold phase (F in a glacial climatic stage; stadial), increasing of Na^+ concentration occurred clearly, like in other fol-

lowing cold stage (stadials), but the concentration increase of aerosol materials such as Ca^{2+} , Mg^{2+} and NO_3^- did not occur, as seen in Fig. 18b. The reason is not completely clear but it can be imagined that the source areas for these chemical materials are not yet completely active at this early stage of the ice sheet formation in the glacial period, although the transportation process are operating

(2) The two peaks pattern of NO_3^- in two glacial period is predominant but it is not seen in the oldest glacial period represented in the records (Figs. 18b and 19). Is this missing peak in the oldest glacial period, due to some climatic or orbital reason or the occurrence of mis-

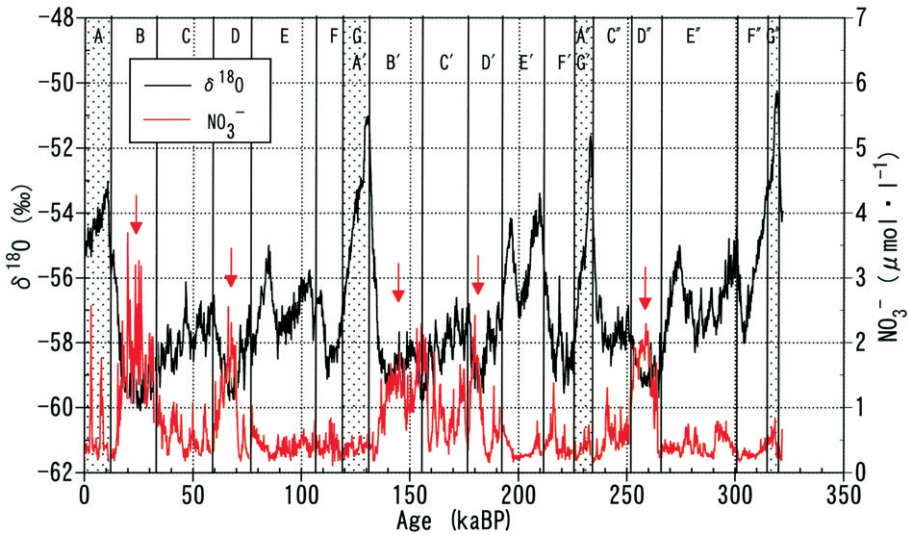


Fig. 19. Occurrence characteristics of concentration profile of NO_3^- during the three glacial-interglacial cycles. Concentrations of NO_3^- are increased in climate stages B and D marked by arrows. $\delta^{18}\text{O}$ is also plotted in this figure.

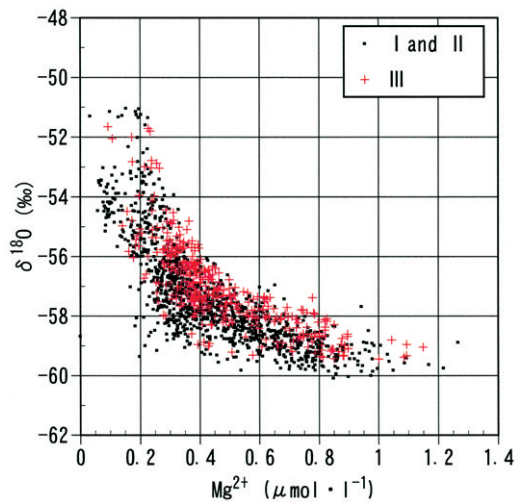


Fig. 20. Mg^{2+} - $\delta^{18}\text{O}$ relation in three glacial-interglacial cycles.

ing layer (long term hiatus) due to lack of sedimentation or decrease of accumulation under a peculiar climatic condition? According to the relation between NO_3^- and $\delta^{18}\text{O}$, the pattern indicate that for the NO_3^- , SO_4^{2-} , Ca^{2+} group, as described before, the NO_3^- concentration increased intensively at a $\delta^{18}\text{O}$ value of -57‰ or lower. This means that insufficient cooling may be an appropriate reason.

(3) Characteristics of the relation between the chemical concentrations and $\delta^{18}\text{O}$ in each “glacial period” of Mg^{2+} and other constituents are shown in Fig. 20. A tendency toward higher concentration in the oldest glacial period is found. It is not clear if this tendency depends on climatic characteristics or/and on physical processes under glacial dynamic condition. This is an important problem for future study.

Acknowledgments

This work is a contribution of the Dome Fuji deep drilling project. We thank all of the colleagues of the glaciological program in the Japanese Antarctic Research Expedition. We also extend our thanks to Mrs. T. Kobayashi, Mrs. Y. Nagamoto, Mrs. M. Naka and Miss M. Nakata for their efforts on the core sample measurements. This work was supported by a Grant-in-Aid for Science Research (No. 10204101) from the Ministry of Education, Culture, Sports, Science and Technology, Japan.

References

- Ageta, Y., Kamiyama, K., Okuhira, F. and Fujii, Y. (1989): Geomorphological and glaciological aspects around the highest dome in Queen Maud Land, Antarctica. *Proc. NIPR Symp. Polar Meteorol. Glaciol.*, **2**, 88–96.
- Barnola, J.M., Raynaud, D., Korotkevich, Y.S. and Lorius, C. (1987): Vostok ice core provides 160,000-year record of atmospheric CO_2 . *Nature*, **329**, 408–414.
- Craig, H. (1961): Isotopic variations in meteoric waters, *Science*, **133**, 1702–1703.
- Dansgaard, W. (1964): Stable isotopes in precipitation, *Tellus*, **16**, 436–468.
- Fujii, Y., Kohno, M., Motoyama, H., Matoba, S., Watanabe, O., Fujita, S., Azuma, N., Kikuchi, T., Fukuoka, T. and Suzuki, T. (1999): Tephra layers in the Dome Fuji (Antarctica) deep ice core. *Ann. Glaciol.*, **29**, 126–130.
- Fujii, Y., Kohno, M., Matoba, S., Motoyama, H. and Watanabe, O. (2003): A 320 k-year record of microparticles in the Dome Fuji, Antarctica ice core measured by laser-light scattering. *Mem. Natl. Inst. Polar Res., Spec. Issue*, **57**, 46–62.
- Japan Meteorological Agency (1996): Antarctic meteorological data at Syowa Station and Dome Fuji Station in 1995. *Antarct. Meteorol. Data*, **36**, 358p.
- Japan Meteorological Agency (1997): Antarctic meteorological data at Syowa Station and Dome Fuji Station in 1996. *Antarct. Meteorol. Data*, **37**, CD-ROM.
- Japan Meteorological Agency (1998): Antarctic meteorological data at Syowa Station and Dome Fuji Station in 1995. *Antarct. Meteorol. Data*, **38**, CD-ROM.
- Johnsen, J., Clausen, H.B., Dansgaard, W., Fuhrer, K., Gundestrup, N., Hammer, C.U., Iversen, P., Jouzel, J., Stauffer, B. and Steffensen, J.P. (1992): Irregular glacial interstadials recorded in a new Greenland ice core. *Nature*, **359**, 311–313.
- Kamiyama, K., Ageta, Y. and Fujii, Y. (1989): Atmospheric and depositional environments traced from unique chemical compositions of the snow over an inland high plateau, Antarctica. *J. Geophys. Res.*, **94**, 18515–18519.
- Kawamura, K. (2000): Variations of atmospheric components over the past 340000 years from Dome Fuji deep ice core, Antarctica. Ph.D. thesis, Tohoku University.
- Kawamura, K., Nakazawa, T., Aoki, S., Nakata, H., Sugawara, S., Fujii, Y. and Watanabe, O. (2003): Atmospheric CO_2 variation over the last three glacial-interglacial climatic cycles deduced from the Dome Fuji deep ice

- core, Antarctica, using a wet extraction technique. *Tellus*, **55B**, 126–137.
- Legrand, M. and Delmas, R.J. (1988) : Formation of HCl in the Antarctic atmosphere. *J. Geophys. Res.*, **93** (D6), 7153–7168.
- Legrand, M. R., Lorius, C., Barkov, N. I. and Petrov, V. N. (1988): Atmospheric chemistry changes over the last climatic cycle (160,000 yr) from Antarctic ice. *Atmos. Environ.*, **22**, 317–331.
- Lorius, C., Jouzel, J., Ritz, L., Merlivat, N., Barkov, N.I., Korotkevich, Y.S. and Kotlyakov, V.M. (1985): A 150,000-year climatic record from Antarctic ice. *Nature*, **316**, 591–596.
- Merlivat, L. and Jouzel, J. (1979): Global climate interpretation of the Deuterium-Oxygen 18 relationship for precipitation. *J. Geophys. Res.*, **84**, 5029–5033.
- National Institute of polar Research (2001): Antarctica: East Queen Maud Land, Enderby Land Glaciological Folio. Tokyo.
- Petit, J., Jouzel, J., Raynaud, D., Barkov, N.I., Barnola, J. M., Basile, L., Bender, M., Chappellaz, J., Davis, J., Delaygue, G., Delmotte, M., Kotlyakov, V. M., Legrand, M., Lipenkov, V.Y., Lorius, C., Pepin, L., Ritz, C., Saltzman, E. and Stievenard, M. (1999): Climate and atmospheric history of the past 420,000 years from the Vostok ice core, Antarctica. *Nature*, **399**, 429–436.
- Satow, K., Watanabe, O., Shoji, H. and Motoyama, H. (1999): The relationship among accumulation rate, stable isotope ratio and temperature on the plateau of east Dronning Maud land, Antarctica. *Polar Meteorol. Glaciol.*, **13**, 43–52.
- Vimeux, F., Masson, V., Delaygue, G., Jouzel, J., Petit, J. R. and Stievenard, M. (2001): A 420,000 year deuterium excess record from East Antarctica: Information on past changes in the origin of precipitation at Vostok. *J. Geophys. Res.*, **106**, 31863–31873.
- Watanabe, O., Kamiyama, K., Motoyama, H., Igarashi, M., Matoba, S., Shiraiwa, T., Yamada, T., Shoji, H., Kanamori, S., Kanamori, N., Nakawo, M., Ageta, Y., Koga, S. and Satow, K. (1997a): A preliminary reports on analyses of melted Dome Fuji core obtained in 1993. *Proc. NIPR Symp. Polar Meteorol. Glaciol.*, **11**, 14–23.
- Watanabe, O., Fujii, Y., Motoyama, H., Furukawa, T., Shoji, H., Enomoto, H., Kameda, T., Narita, H., Naruse, R., Hondoh, T., Fujita, S., Mae, S., Azuma, N., Kobayashi, S., Nakawo, M. and Ageta, Y. (1997b): A preliminary study of ice core chronology at Dome Fuji Station, Antarctica. *Proc. NIPR Symp. Polar Meteorol. Glaciol.*, **11**, 9–13.
- Watanabe, O., Kamiyama, K., Motoyama, H., Fujii, Y., Shoji, H. and Satow, K. (1999): The paleoclimate record in the ice core at Dome Fuji station, East Antarctica. *Ann. Glaciol.*, **29**, 176–178.
- Watanabe, O., Shoji, H., Satow, K., Motoyama, H., Fujii, Y., Narita, H. and Aoki, S. (2003): Dating of the Dome Fuji, Antarctica deep ice core. *Mem. Natl Inst. Polar Res., Spec. Issue*, **57**, 25–37.

(Received December 12, 2002; Revised manuscript accepted February 3, 2003)